

RSC Advances



This article can be cited before page numbers have been issued, to do this please use: A. B. Volikov, S. Ponomarenko, A. Gutsche, H. Nirschl, K. Hatfield and I. V. Perminova, *RSC Adv.*, 2016, DOI: 10.1039/C6RA08636E.



This is an *Accepted Manuscript*, which has been through the Royal Society of Chemistry peer review process and has been accepted for publication.

Accepted Manuscripts are published online shortly after acceptance, before technical editing, formatting and proof reading. Using this free service, authors can make their results available to the community, in citable form, before we publish the edited article. This *Accepted Manuscript* will be replaced by the edited, formatted and paginated article as soon as this is available.

You can find more information about *Accepted Manuscripts* in the [Information for Authors](#).

Please note that technical editing may introduce minor changes to the text and/or graphics, which may alter content. The journal's standard [Terms & Conditions](#) and the [Ethical guidelines](#) still apply. In no event shall the Royal Society of Chemistry be held responsible for any errors or omissions in this *Accepted Manuscript* or any consequences arising from the use of any information it contains.

1 **Targeted design of water-based humic substances-silsesquioxane soft materials**
 2 **for nature-inspired remedial applications**

3
 4 Alexander B. Volikov,^a Sergei A. Ponomarenko,^{a,b,} Alexander Gutsche,^c Hermann Nirschl,^c Kirk
 5 Hatfield,^d Irina V. Perminova^{a**}

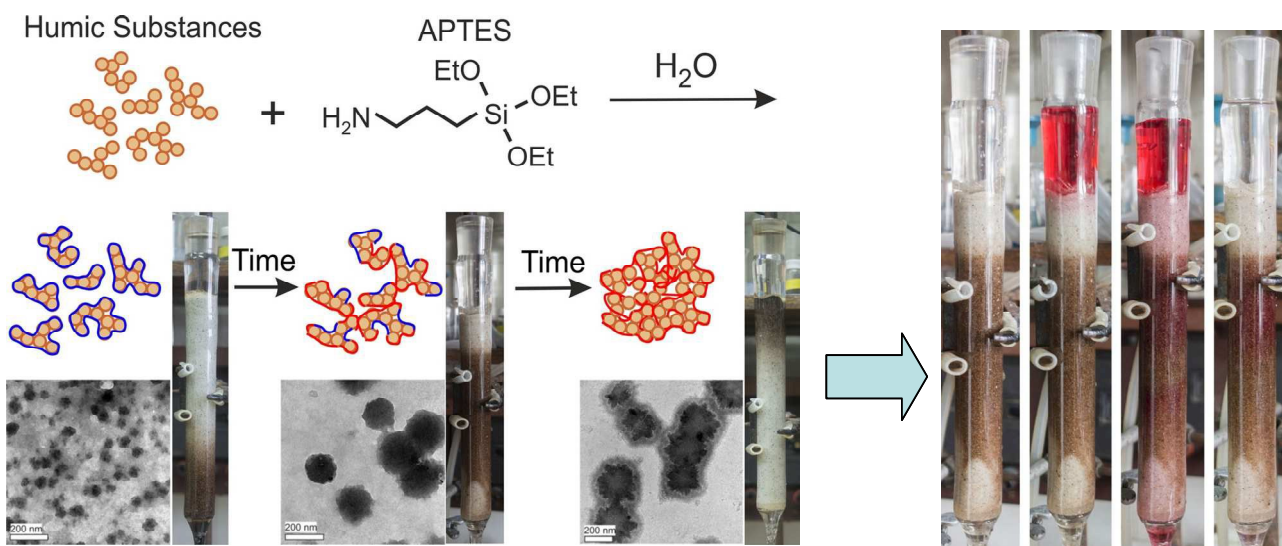
6 ^a Department of Chemistry, Lomonosov Moscow State University, Moscow, Russia;

7 ^c Enikolopov Institute of Synthetic Polymeric Materials of Russian Academy of Sciences, Moscow,
 8 Russia;

9 ^c Institute for Mechanical Process Engineering and Mechanics, Karlsruhe Institute of Technology
 10 (KIT), Karlsruhe, Germany;

11 ^d Engineering School for Sustainable Infrastructure and Environment, University of Florida,
 12 Gainesville, USA

13



* Corresponding Author: Phone/fax: +7 495-939-5546; e-mail: ipermin@org.chem.msu.ru

16 Water-based humic substances-silsesquioxane (HS-SQ) soft materials are synthesized by
17 hydrolysis of (3-aminopropyltriethoxy)-silane in the HS solution. The aggregation dynamics of this
18 system was studied using in situ small-angle X-ray scattering (SAXS) technique, which revealed
19 three consecutive stages in the evolution of the HS-SQ system in time based on its fractal dimension
20 (D): HS-SQ oligomeric polyelectrolyte complexes with $D < 2.5$; loosely bound HS-SQ networks with
21 $2.5 < D < 3.0$, and densely cross-linked networks with $D > 3$ (surface fractals). It was suggested that the
22 reaction time needed for the HS-SQ system to transit from mass to surface fractal stage can be used
23 to control its self-assembly onto a solid support. The corresponding studies have confirmed that the
24 HS-SQ networks could be successfully immobilized onto sand columns only at the aggregation
25 stage with fractal dimensions of $2.5 < D_m < 3$. This enabled the targeted design of the HS-SQ systems
26 capable of guided self-assembly onto the solid support. The corresponding lab column studies have
27 demonstrated successful passive installation of humic permeable reactive barrier on sand which was
28 capable of intercepting azo dye from the contaminated water. Prospects of using HS-SQ soft
29 materials in nature-inspired remedial technologies and soil restoration are discussed.

30

31 1. INTRODUCTION

32 Humic substances (HS) are natural hyperbranched polyelectrolytes of acidic character resulting from
33 the presence of numerous carboxyl groups in their structure. They occur throughout the environment
34 and perform multiple life-sustaining functions in soil and water.¹ Of particular importance are their
35 multiple roles in natural attenuation of environmental pollution. For example, HS tend to accumulate
36 onto mineral surfaces such as suspended sediments that settle in aquatic environments and form
37 organic-rich geochemical barriers in stream and lake beds that act as efficient geosorbents for metals
38 and organic compounds.^{2,3} And as another example, when dispersed in oil-contaminated water,
39 humic-modified fine particles can self-assemble into colloidosomes, known as oil-suspended matter

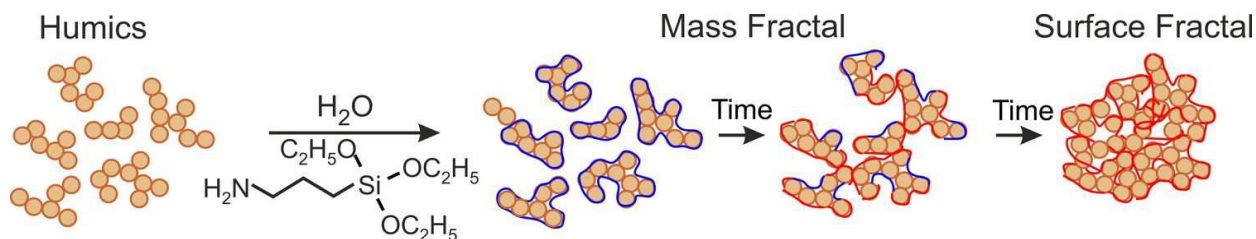
40 aggregates (OSA): this process governs the natural remediation of oil contaminated sediments in
41 coastal environments.^{4,5} Hybrid porous materials, represented by soil aggregates, play a crucial role
42 in both protecting organic carbon and water retention capacity of soils.⁶ Hence, acquiring control
43 over the self-assembly of humic polyelectrolytes, spanning in sizes from 400 to 100000 Da, onto the
44 mineral surfaces could present opportunities to develop nature-inspired solutions for environmental
45 remediation and sustainable agriculture.

46 In this context, incorporation of silanol functionalities into humic molecules looks
47 particularly promising due to the high affinity of silanols to mineral surfaces. Recently, we have
48 demonstrated that silanol-modified humic materials can be sorbed in large quantities (up to 200
49 mg/g) onto hydroxylated solid supports with well developed surfaces like silica gel and clay.^{7,8}
50 These derived materials demonstrated significantly elevated sorption capacities for organic
51 contaminants (e.g., diazodyes) comparable to that of activated carbon.⁸ Similar hybrid sorbents with
52 immobilized humic layers were described by other authors as well.⁹⁻¹² Still, these lab-prepared solid
53 sorbents do not meet the challenge of achieving in situ aquifer remediation with injectable reactive
54 barriers (i.e., without excavating contaminated soils or sediments).^{13,14} The same is true for restoring
55 the humus content in soils which implies the in situ immobilization of large quantities of organic
56 matter onto soil minerals. To meet these demands, polymer-like soft materials should be developed
57 capable of self assembly into cross-linked networks upon the contact with solid supports (including
58 those with limited surface development, such as sand). We hypothesized that water-based humic
59 substances-siloxane networks could be used for these purposes.

60 To prove this hypothesis, we have studied the dynamics of cross-linking and aggregation of
61 3-aminopropyltriethoxysilane (APTES) in the HS solution under varying reaction conditions using
62 the in situ small angle X-ray scattering (SAXS) technique. It provided the unique possibility to
63 monitor the progressive cross-linking of the HS-APTES system over time from loosely linked

64 aggregates with mass fractal dimension towards more densely packed aggregates with surface fractal
65 dimension as it is schematically shown in Fig. 1.

66



68 **Fig 1** Schematic interactions between HS and 3-aminopropyltriethoxysilane leading to the formation
69 of aggregates described with fractal dimensions of mass and surface fractals.

70

71 Given that APTES is composed of triethoxygroup attached to aminopropyl-radical, the
72 products of its polymerization fall under definition of silsesquioxanes (SQ). The latter refers to all
73 structures with the empirical formulas $\text{RSiO}_{3/2}$ where R is hydrogen or any alkyl, alkylene, aryl,
74 arylene, or organo-functional derivatives of alkyl, alkylene, aryl, or arylene groups.^{15,16} We have
75 demonstrated that the HS-SQ network possessed maximum functionality with respect to
76 immobilization onto solid support prior to its transition from mass to surface fractal state. This
77 provided theoretical backgrounds for application of the developed HS-SQ soft materials capable of
78 passive in situ immobilization on solid support (e.g. sand). The sorption performance of the
79 immobilized HS-SQ networks was demonstrated with respect to model contaminant – azo dye. This
80 indicated for the promising perspectives for the in situ applications of HS-SQ networks both for
81 installing “soft matter” reactive barriers in the contaminated aquifers and for increasing the content
82 of humified matter in the organics-depleted soils.

83

84 2. EXPERIMENTAL

85 2.1. Humic Materials

86 Coal humic acid (CHP) was prepared by desalination of the potassium humate from leonardite
87 (Powhumus; Humintech Ltd., Germany). It was characterized by the following elemental
88 composition (% mass on ash-free basis): C - 53.4, H - 5.15, N - 1.31, S -2.36, O - 37.8; and content
89 of carboxylic groups (mmol g⁻¹): 4.1. For preparation of HS solutions, a weight of CHP was ionized
90 by few drops of 3M NaOH, diluted with distilled water, and then adjusted to a desired pH using 1M
91 HCl. All reagents used for this purpose were of analytical grade. Concentration of CHP in
92 experiments solutions varied from 1 to 10 g·L⁻¹.

93

94 2.2. Humic Substances -Silsequioxane Networks Synthesis

95 3-aminopropyltriethoxy-silane was purchased from Carl Roth GmbH, Germany. It was used to
96 create different APTES:CHP ratios in solution which varied from 1:4 to 2:1 by weight. APTES was
97 added dropwise to the experimental solution of CHP under continued stirring. pH of the CHP-
98 APTES solution was adjusted using 1M HCl, and the total volume was made up to 10 mL using
99 distilled water. The reaction flask was then hermetically sealed and fixed onto overhead shaker. The
100 experimental solution was then aged and periodically sampled for kinetic measurements using in
101 situ SAXS technique.

102

103 2.3. In situ SAXS and Transmission Electron Microscopy (TEM)

104 The SAXS experiments were conducted by means of a modified Kratky camera at the Institute of
105 Mechanical Process Engineering and Mechanics (MVM) of Karlsruhe Institute of Technology
106 (KIT). The camera was equipped with a copper anode (X-ray tube KFL Cu, line focus 0.4×12 mm,

107 Siemens, X-ray generator Kristalloflex 760 Bruker AXS). A photosensitive imaging plate was used
108 as detector. The samples (0.3 mL) were placed in a quartz capillary and irradiated for three minutes.
109 A detailed description of the camera and the data evaluation are described previously.¹⁷

110 TEM images were acquired using a Philips CM 12 microscope operating at 120 kV. For
111 these measurements carbon-coated grids were briefly dipped into the solution and dried under air.

112 2.4. Analysis of Scattering Data

113 The SAXS method is based on the elastic scattering of X-rays at electrons. In a homogeneous
114 medium, the intensity of the scattered X-rays (I) is accordance a function of the scattering vector (q).

115 For a system of N identical particles, the scattering occurs in with the Guinier law:

$$116 \quad I(q) = N(\Delta\rho^2)V^2 \exp\left(-\frac{q^2 R_g^2}{3}\right) \quad (1)$$

117 where R_g is the gyration radius of the particles of volume V , and $\Delta\rho$ is the difference in electronic
118 density between the particles and the dispersion medium. The Guinier law is valid as long as R_g is
119 small enough (for the range $0 < q < 1/R_g$). From equation 3, the radius of gyration may be found
120 from the slope of a plot of $I(q)$ versus q^2 .

121 For larger q , the scattering intensity typically decreases according to a power law. In the
122 power law regime, the concept of fractal geometry can be used to determine structural information
123 on fractals.^{18, 19} Scattering in this regime depends on the geometric structure of the particles in the
124 system. Fresh gels frequently exhibit mass fractal structures. The SAXS intensity from a mass
125 fractal structure shows a power law dependence on q :

$$126 \quad I(q) \sim q^{-D_m} \quad (2)$$

127 The fractal dimension $1 < D_m \leq 3$ can be obtained from the slope of a $\log I$ vs. $\log q$ plot. In case of
128 surface fractals which exhibit a compact interior and a fractal surface of lower density, the power
129 law shows an exponent $3 < 6 - D_s \leq 4$, i.e.

$$I(q) \sim q^{-(6-D_s)} \quad (3)$$

131 Once the exponent is known, the surface fractal dimension, D_s , can be readily calculated.

132

133 **2.5. Immobilization of the HS-SQ Networks on Solid Support**

134 The glass columns prepacked with 100 mL of quartz sand were used for dynamic sorption. Prior to
135 use, the column was washed with 2 L of distilled water (MilliQ). A solution of potassium humate
136 CHP was prepared at the concentration of $5 \text{ g}\cdot\text{L}^{-1}$, and 20 mL were transferred into a beaker. A
137 needed aliquot of APTES (50, 100, or 200 μl) was added to the beaker under continued stirring to
138 obtain HS-SQ networks with different CHP:APTES ratios: 1:0.5, 1:1 and 1:2 (w:w) which were
139 designated as CHP-APTES-50, CHP-APTES-100, and CHP-APTES-200, respectively. Then pH
140 value was adjusted to 8 using 1M HCl and the mixture was aged for 120 min in case of CHP-
141 APTES-50, for 40 minutes in case of CHP+APTES-100, or immediately introduced into the column
142 in case of CHP-APTES-200.

143 Each of the aged CHP:APTES mixtures in a volume of 20 mL was quickly introduced into a
144 sand column at an elution rate of 10 mL per minute, then 10 mL of distilled water was added at the
145 same rate to place the mixture in the center of the column. After that the column was hooked up to a
146 flask with distilled water, the flow rate was set to 5 mL per hour, and flushed overnight. Then the
147 column was washed with distilled water at 1 mL per minute to remove the residues of non-reacted
148 mixture. Concentration of not-sorbed HS was determined spectrophotometrically at the absorption
149 wavelength of 254 nm. The content of immobilized HS was calculated as a difference between
150 introduced and recovered amount of HS. To remove the immobilized HS-SQ network, 0.01 M
151 NaOH (300 mL) was used to flush the column, which desorbed the HS-SQ network from the sand.

152

153 2.6. Dynamic Sorption Experiments with Azo Dye Direct Red 81

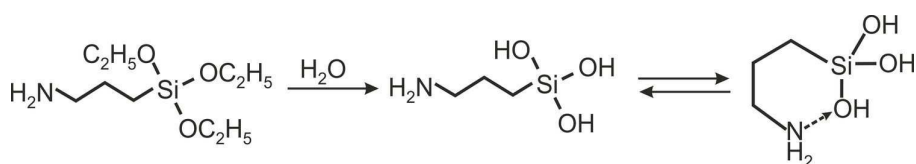
154 Direct Red 81 diazo dye (molecular formula $C_{29}H_{19}N_5Na_2O_8S_2$, CAS Registry Number: 2610-11-
155 9/12237-71-7) was used as a model contaminant. The dye solution in distilled water at a
156 concentration of $25 \text{ mg}\cdot\text{L}^{-1}$ was passed through the sand column with the immobilized HS-SQ
157 materials prepared as described above at an elution rate of $1.3 \text{ mL}\cdot\text{min}^{-1}$ until the column was
158 exhausted. The HS-SQ networks with CHP:APTES ratios of 2:1, 1:1, and 1:2 were immobilized on
159 sand. The void volume of the column was 48 mL. The breakthrough curves of the azo dye were
160 detected by measuring optical density of the solution exiting the column at a wavelength of 511 nm.

161

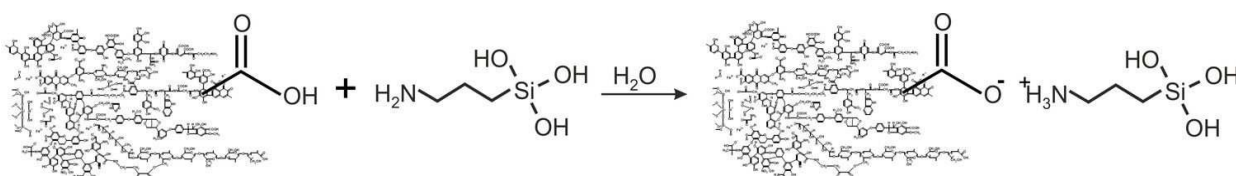
162 3. RESULTS AND DISCUSSION

163 3.1. Synthesis of Water-Based Humic Substances –Silsesquioxane networks

164 Upon designing synthesis of water-based HS-SQ networks, we used the unique property of 3-
165 aminopropyltrialkoxysilanes (APTS) to produce rather stable solutions in water due to formation of
166 cyclic intermediates as it is shown below:^{20,21}



168 This is unlike other functional organosilanes, which polymerize rather quickly in water with
169 formation of insoluble precipitates of polysiloxanes. Hence, to initiate polymerization of APTS in
170 water, it was necessary to prevent formation of these cyclic intermediates. To achieve that we used
171 negatively charged humic polyanions whose carboxylic functionalities were to outcompete silanols
172 in binding with amine groups as it is shown in the following reaction for 3-
173 aminopropyltriethoxysilan (APTES) used in our studies:



174

175 In this case free silanol groups were to start interacting with each other by forming intra- and inter-
 176 particle silsesquioxane structures $(\text{SiO}_{3/2})_n$. We have conducted the corresponding reactions at
 177 different pHs, reagent ratios, concentration of HS, and in the presence of calcium ions. The
 178 motivation was to reveal the primary factors controlling the rate of humic-siloxane network self-
 179 assembly and their immobilization properties.

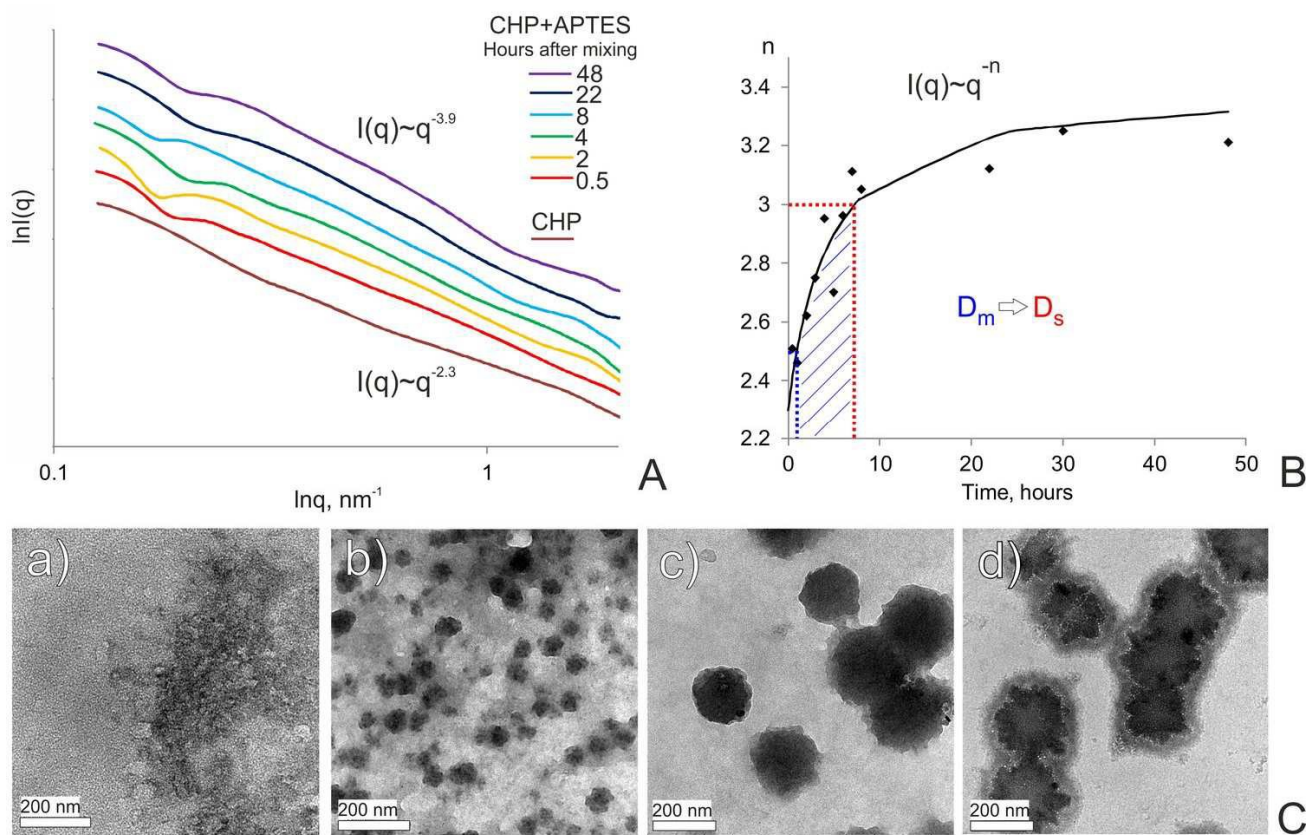
180

181 3.2. In situ SAXS Studies of the Aggregation Dynamics of the Aqueous HS–SQ Systems.

182 The SAXS data were acquired over 48 hours after APTES was added to solution of CHP sample. A
 183 typical set of SAXS curves is shown in Fig. 2A, the corresponding plot of the power law exponent n
 184 versus reaction time is presented in Fig. 2B, and TEM-images of the CHP-APTES system at 0, 1, 4
 185 and 22 hours reaction time are shown in Fig. 2C.

186 The SAXS curve of initial solution of CHP did not show any characteristic peaks as
 187 indicated by the linearity in log-log plot (Fig. 2A). Its fractal dimensions varied between 2.2 and 2.4,
 188 which is indicative that HS in the solution exist as mass fractals producing loose soft networks
 189 without a hard core. The resultant D_m values were consistent with the reported findings.^{22,23} The
 190 minimum observed D_m values were at an alkaline pH (2.2 at pH 9), whereas a decrease in pH led to
 191 an increase in D_m up to 2.4 at pH 4. This could be explained if HS aggregation were enhanced under
 192 acidic pH conditions due to smaller overall charge and pronounced intramolecular hydrogen
 193 bonding. Similar effects were reported in earlier works.^{24,25} The presence of Ca^{2+} ions in the system
 194 caused an increase in D_m value for CHP up to 2.5, which was to expect, because HS readily react
 195 with calcium ions which promotes their aggregation.²⁶ (The results are shown in the ESI).

196



197

198 **Fig 2** Evolution of the CHP-APTES system (1:1 ratio (w:w), 5 g·L⁻¹ CHP, pH 8) over reaction time.

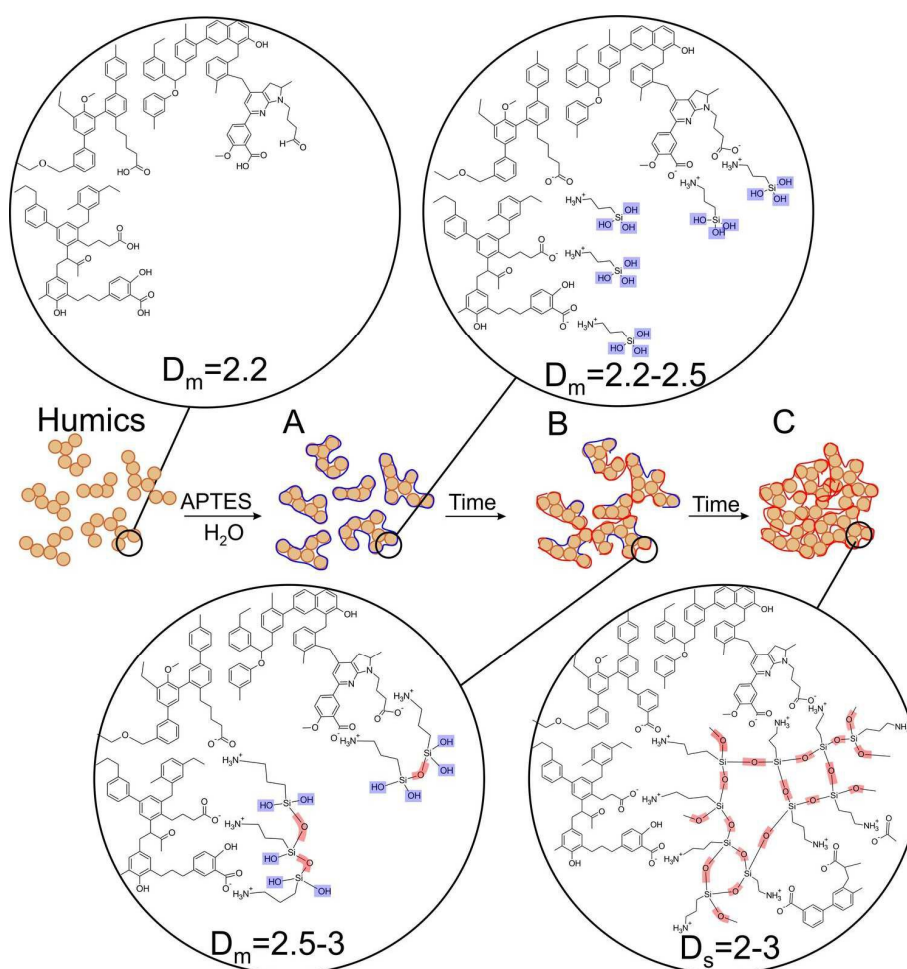
199 A) SAXS curves at different reaction times (hours) coded with colors: red – 0.5, yellow – 2, green –
 200 4, cyan – 8, violet – 22, purple – 48), initial CHP solution - brown; B) dependence of the slope of
 201 log-log plots shown in Fig. 2a on time. Shaded area denotes mass fractal range, transition time of
 202 mass to surface fractals (D_m to D_s , respectively) is shown with a red bar; C) TEM images of CHP-
 203 APTES system after 0, 1, 4, and 22 hours of reaction time: a, b, c, and d, respectively.

204

205 The addition of APTES to CHP solution caused a steep increase in a value of fractal
 206 dimension (Fig. 2B) which is indicative of substantial aggregation processes occurring in the
 207 system. It means that in the course of the CHP-APTES interaction larger aggregates are formed.
 208 This process leads to formation of denser core and more porous periphery which is reflected as an

209 increase in fractal dimension. In the low- q regime, a local minimum was observed. Fitting of the
210 corresponding data by means of eq 3 did not yield reasonable estimates of the gyration radius of the
211 scattering particles. This may indicate that the formed particles were larger than 40-50 nm, which is
212 the upper structural limit of the SAXS camera used in our studies. Hence, the observed inflection
213 might be referred to inter-aggregate scattering of X-rays resulting from high concentration of humic-
214 siloxane particles. This explanation is in line with the TEM data (Fig. 2C) which show that already
215 at the beginning of the reaction the particles were on the order of 50-70 nm. Then, in the course of
216 APTES condensation, the dense polysilsesquioxane particles were formed which coalesced into
217 larger particle aggregates with sizes 150 -250 nm

218 As it can be deduced from Fig. 2, in the course of the first hour of the reaction, mostly
219 formation of APTES-HS polyelectrolyte complexes occurs with the fractal dimension close to that
220 of the initial CHP solution. Then, they undergo speedy aggregation followed by an increase in mass
221 fractal dimension from 2.3 up to 3.0. These mass fractals transition further into the surface fractals.
222 The transition of mass to surface fractals can be explained by the fact that the aminoorganosilane
223 bound to humic molecules continued to polymerize in water producing polysilsesquioxane bonds
224 resulting in formation of much denser particles as compared to initial “fluffy” aggregates. These
225 dense particles continued to interact with each other producing aggregates of particles with much
226 smoother surface as compared to initial particles. This process is then reflected as a decrease of the
227 surface fractal dimension of these aggregates (from $D_s = 2.7$ down to $D_s = 2.1$). The obtained X-ray
228 scattering data and TEM imaging allowed us to propose conceptual model of the HS-SQ network
229 formation which is shown in Fig. 3.



230

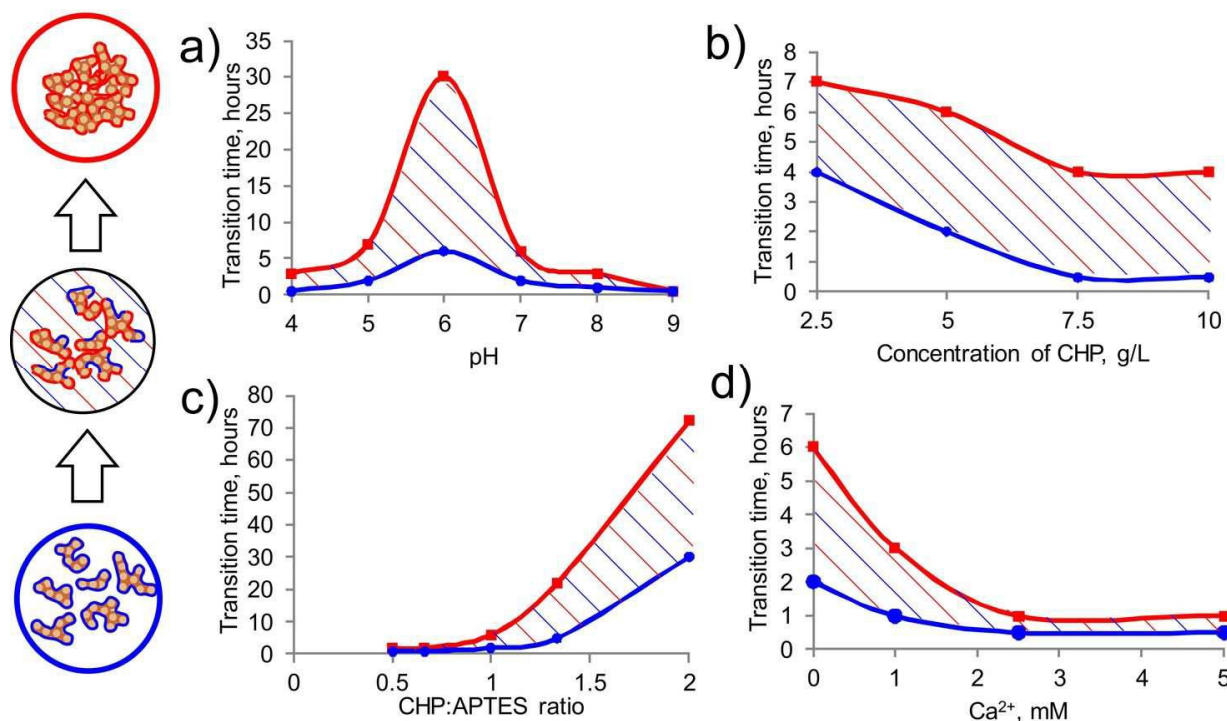
231 **Fig. 3** Conceptual model of the water-based HS-SQ network formation and evolution in time: The
 232 first insert shows a fragment of HS network with D_m of 2.2, A) shows formation of CHP-APTES
 233 complexes rich in silanol groups (marked in blue) with low D_m values, B) shows initial siloxane
 234 bonding (marked in red) resulting in aggregate formation with high D_m values, C) shows branched
 235 silsesquioxane cross-linking (D_m to D_s transition).

236

237 3.3. SAXS studies on dynamics of the CHP:APTES system under different reaction conditions

238 To acquire further experimental evidence to the proposed aggregation mechanism, we have probed
 239 the dynamics of the CHP:APTES system in time under different reaction conditions by changing
 240 pH, reagent ratios, concentration of HS and Ca ions. Overview of the results of in situ SAXS

241 responses to the above parameters are summarized in Fig. 4 and detailed data are summarized in
242 Tables S1-S4 in the ESI.



243

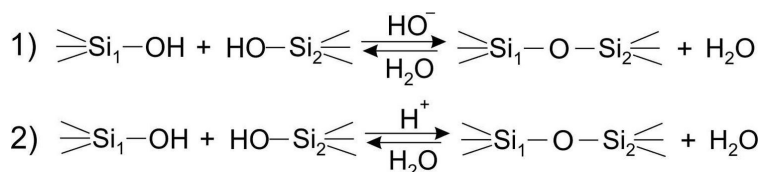
244 **Fig 4** The dependence of the transition time of the mass to surface fractals conversion in the CHP-
245 APTES system (highlighted in red), and of the time needed to reach the mass fractal dimension D_m
246 = 2.5 (highlighted in blue) on different reaction parameters: a) pH (CHP:APTES=1:1, CHP
247 concentration = $5 \text{ g}\cdot\text{L}^{-1}$, $[\text{Ca}^{2+}] = 0$); b) concentration of CHP (pH=7, CHP:APTES = 1:1, $[\text{Ca}^{2+}] = 0$, c)
248 the ratio of CHP:APTES (pH=7, CHP concentration = $5 \text{ g}\cdot\text{L}^{-1}$, $[\text{Ca}^{2+}] = 0$); d) concentration of Ca^{2+}
249 (pH=7, CHP:APTES = 1:1, CHP concentration = $5 \text{ g}\cdot\text{L}^{-1}$).

250

251 It can be seen that the HS-SQ system behaved in a similar manner over a broad pH range in a
252 sense that the mass fractals were formed at the initial interaction stage, which were further
253 transformed into the surface fractals (Fig. 4A). The observed transformation did not imply a phase
254 transition, but it was accompanied by a substantial change in the material properties, such as

255 porosity, surface area, and activity, which decreased along with a transition of mass to surface
 256 fractals. Hence, the time needed for such a transition can serve as a characteristic parameter of the
 257 system to control or even exploit its functional properties. From this point of view it is of
 258 importance to note that the maximum transition time from mass to surface fractals (30 hours) was
 259 characteristic to the CHP-APTES system with initial pH 6, which corroborates well the silicon
 260 chemistry: the minimum hydrolysis and siloxane bond formation rate at pH 6.²⁸⁻³⁰

261 A decrease in this transition time (which is equivalent to the higher hydrolysis and siloxane
 262 formation rate) was observed both along with acidification of the system (2 hours at pH 4) and even
 263 more with the alkanization of the system (immediately at pH 9). This behavior can be explained by
 264 acidic and basic catalysis of the hydrolytic processes which undergo organoalkoxysilanes in aqueous
 265 solutions which is schematically shown below:³⁰



267 This is a reason that an impact of other parameters on formation of humic-siloxane networks,
 268 was examined at pH 7 and varied concentrations of HS, Ca, and the reagent ratio (CHP:APTES).

269 Concentration of HS had less pronounced effect on the polymerization rate as compared to a
 270 change in pH value (Fig. 4B). Still, its increase accelerated the transition of the system from mass to
 271 surface fractal state. Much more significant was the reagent ratio (CHP:APTES). An increase in
 272 APTES proportion significantly accelerated the system aging accompanied by transition from mass
 273 to surface fractal particles: at the CHP:APTES ratio of 1:2, it occurred in only 2 hours, whereas at
 274 the 2:1 ratio, the transition took place after 72 hours. The further increase in CHP proportion in the
 275 system (4:1 ratio) slowed down the transition time so dramatically that it was not reached even after
 276 a month of aging time: the fractal dimension did not exceed the D_m value of 2.5. The solution was

277 stable over this month and there was no precipitate observed. An addition of Ca ions has
278 substantially accelerated formation of aggregates (Fig 4D). This corroborates the expected behavior
279 of the system while it is known that calcium promotes aggregation of both HS and APTES in
280 aqueous solutions due to formation of insoluble salts.²⁶ As a result, the HS-SQ network was least
281 stable in the presence of calcium.

282 The relationships found corroborate the conceptual model of the evolution of HS-SQ
283 network proposed in Fig. 3. Their examination suggests that the HS-SQ system under study
284 possesses maximum functionality with regard to its immobilization capacities when it reaches the
285 state of poorly cross-linked large aggregates rich in silanol groups (stage C). This allowed us to
286 define the optimum operational conditions shown with shaded areas in Fig. 4. Within these areas the
287 poorly cross-linked voluminous aggregates are formed rich in silanol groups capable of further
288 cross-linking into 3D polysilsesquioxane networks. This makes those systems the best candidates for
289 immobilizing onto solid supports depleted with surface binding sites, e.g., sand. The key for
290 preparing the CHP-APTES systems with those properties is to use appropriate reaction time (in the
291 range of blue and red lines) for the given reaction conditions.

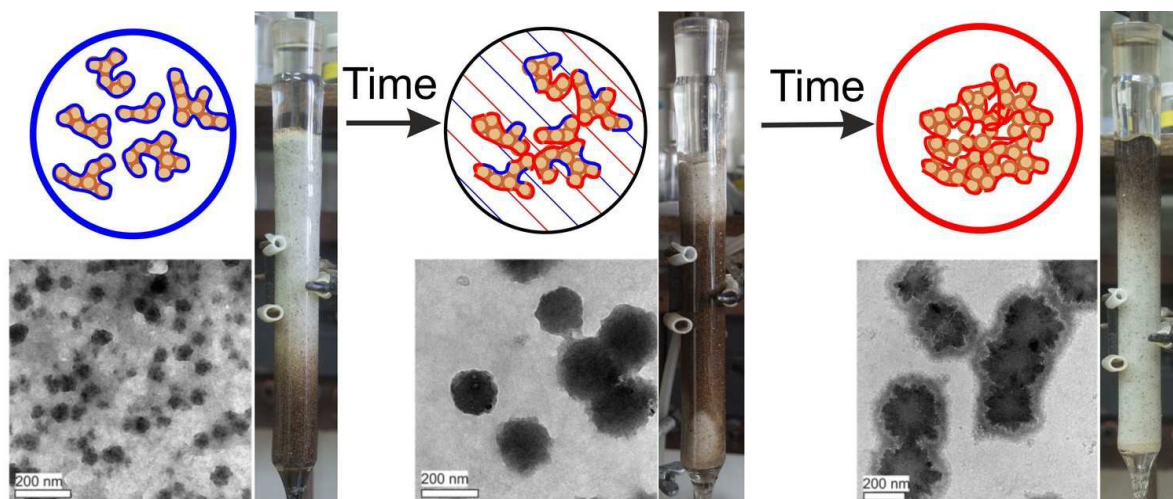
292

293 **3.4. Immobilization of the HS-SQ networks onto the solid supports.**

294 To demonstrate how the aging time of the CHP:APTES mixture before its contact with the solid
295 support impacts the immobilizing performance, we prepared CHP:APTES mixtures at pH 8 and
296 injected them into the column at three different stages of HS-SQ networks formation: 1)
297 immediately after mixing at the stage of interpolyelectrolyte complexes; 2) after aging time which
298 did not exceed the transition time of mass to surface fractals; and 3) after aging time exceeding
299 transition time of mass to surface fractals. We used high elution rates to inject the CHP:APTES
300 mixtures into the middle of the column, then the flow rate was slowed down to approach those of the

301 ground water, and the system was washed continuously with distilled water. The intent was to
302 simulate active injection of the preconditioned HS-SQ network via a borehole followed by its
303 passive migration and immobilization onto the solid support of the aquifer. The immobilization
304 performance of the CHP-APTES system used at different aging times is illustrated in Fig. 5.

305



306

307 **Fig 5** Immobilization of the HS-SQ networks onto the sand column after different aging times
308 (CHP:APTES=1:1, concentration of CHP = $5 \text{ g} \cdot \text{L}^{-1}$, pH 8): A) injected at aging time 0 (immediately
309 after mixing): no retardation on the column; B) injected after 40 min: the humic layer was
310 immobilized in the middle of the column, C) injected after 2 hours: the precipitate was formed and
311 settled in the upper part of the column.

312 These experiments allowed us to determine aging times that provide for best HS-SQ network
313 immobilization at different CHP:APTES ratio (2:1, 1:1, and 1:2) at the given pH 8. For the systems
314 under study they accounted for (in minutes) 120, 40, and 5, respectively, which corroborates with
315 the mass-to-surface fractal transition time determined for the corresponding systems from the
316 scattering data (Fig. 3).

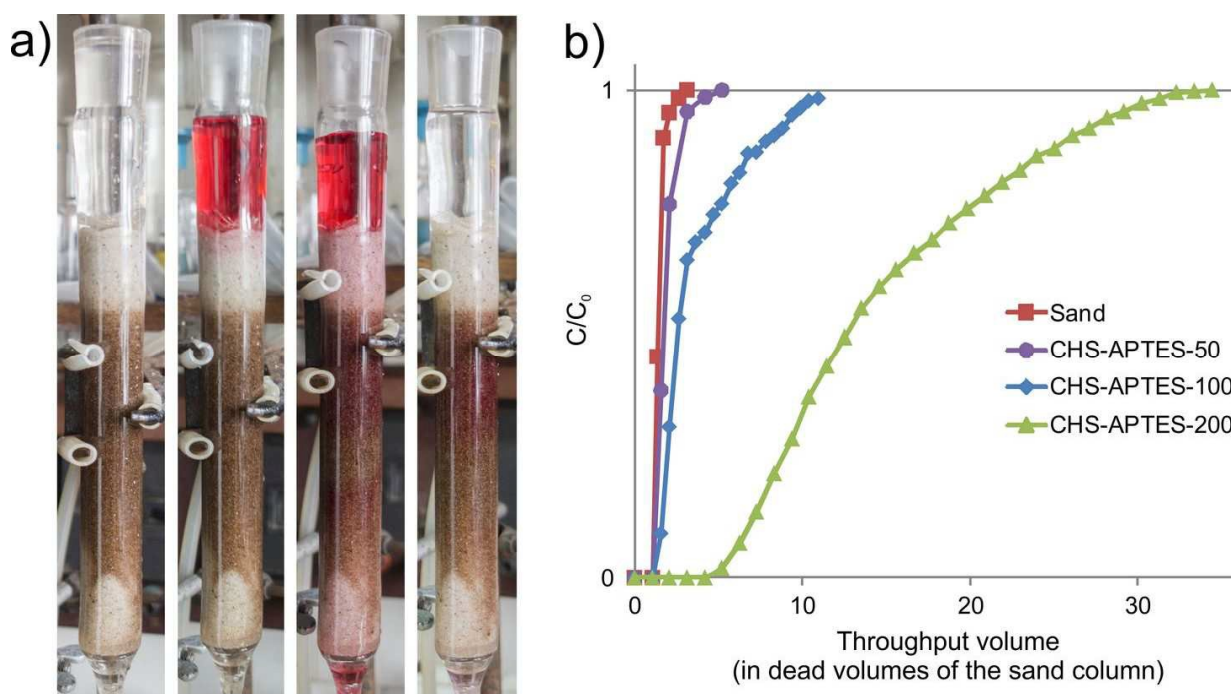
317 A capturing performance of the same HS-SQ networks with three different reagent ratios was
318 estimated based on the amount of the reagent leached from the column. The corresponding values
319 accounted for (in % of the introduced mass) 21, 81, and 96 for the CHP:APTES systems with
320 reagent ratios of 2:1, 1:1, and 1:2, respectively (the data are presented in Table 1). This indicates that
321 an increase in APTES proportion improves performance of the system. Of importance is that the
322 immobilization of the HS-SQ network onto the sand did not impact its hydraulic conductivity.
323 Hence, the developed system has good prospects as a liquid medium for installation of humic
324 permeable reactive barriers (HPRBs) onto granular support of the contaminated aquifers. From
325 technological point of view it was necessary to find a way for removing HPRBs from aquifer
326 support. The corresponding experiments on desorption of HPRB from sand have demonstrated that
327 the HS-SQ system can be completely removed (washed out) from sand by diluted alkali (e.g., 0.01
328 M NaOH). We have found that a switch of washing solution from distilled water to 0.01 M NaOH
329 lead to complete desorption of the HS-SQ network from the sand. In practice it means that a diluted
330 alkali can be pumped in into the installation well; and after desorption of the HS-SQ system it can
331 be pumped out of another well located downstream in the same aquifer. Overall, the results obtained
332 demonstrate a facile in-situ immobilization and removal of HPRB onto granular aquifer support (e.g.
333 sand) using guided self-assembly of the water-based HS-SQ networks.

334 To evaluate functional properties of the immobilized HS-SQ networks with respect to
335 contaminant sequestration, we used the azo dye Direct Red 81, which is a dibasic sodium salt. Given
336 that both the selected azodye and humic polyelectrolytes are negatively charged at neutral pH, we
337 expected increased sorption of the diazodye onto HS-SQ networks with the higher content of
338 positively charged APTES. The corresponding column experiments are shown in Fig. 6A. The
339 sorption isotherms are shown for three different CHP:APTES ratios (Fig. 6B). After the column was
340 saturated with the azo dye, we conducted desorption of azodye using distilled water as an eluent.

341 This was done to estimate amount of azo dye which was strongly bound to the HS-SQ polymers The
342 corresponding sorption-desorption parameters are summarized in the two last columns of Table 1.

343 From Fig. 6 and Table 1 it can be deduced that the azo dye was poorly sorbed on pure sand,
344 but it was retained in much larger quantities by the immobilized HS-SQ materials; moreover, the
345 amount of sorbed azodye increased along with the amount of APTES in the HS-SQ network and
346 with the total amount of the humic material immobilized onto sand.

347



348

349 Figure 6. Dynamic sorption of Direct Red 81 azo dye onto the HS-SQ soft material immobilized in
350 situ onto sand. a) experimental design; b) dynamic isotherms for the CHP:APTES ratios of 2:1, 1:1,
351 and 1:2, highlighted in violet, blue, and green, respectively. Concentration of azodye is $25 \text{ mg}\cdot\text{L}^{-1}$,
352 pH 7, elution rate is $1.3 \text{ mL}\cdot\text{min}^{-1}$, void column volume is 48 mL.

353

354

Table 1. Sorption-desorption characteristics* of the azo dye Direct Red 81 (AD) onto the HS-SQ materials immobilized on sand at different CHP:APTES ratios

Column treatment	Amount of retained CHP, mg	Amount of retained CHP, % of total	Amount of sorbed AD, mg	Amount of desorbed AD, mg
Pure quartz sand	0	0	0.28	0.08
CHP:APTES of 1:2	12	21	1.14	0.23
CHP:APTES of 1:1	68	81	2.84	0.06
CHP:APTES of 2:1	92	96	14.92	3.68

355 *For sorption experiments the elution rate was $5 \text{ mL}\cdot\text{h}^{-1}$, for desorption – $1 \text{ mL}\cdot\text{h}^{-1}$. Desorption was
356 conducted using distilled water.

357

358 This might be indicative of leading electrostatic interactions between the azo dye and the HS-SQ
359 soft material immobilized onto sand: only small amount of dye was sorbed by CHP-APTES-50,
360 which carried overall negative charge (the observed sorption might be referred to hydrophobic
361 binding); whereas much larger amounts of azodye were retained at the CHP-APTES-200 which was
362 characterized by an excess of amino groups of organosilane and carried overall positive charge. The
363 obtained results are in good agreement with the reported data on enhanced sorption of dyes on
364 humics-modified solid sorbents.^{9,12}

365 It should be specifically stressed that as in case of the removal of the immobilized HS-SQ
366 networks from the granular aquifer support, which we discussed above, the sorbed azodye can be
367 also completely removed from the solid support by washing it off with 0.01 M NaOH. In our
368 column experiments we have found that the azodye elutes together with the HS-SQ materials upon
369 washing with 0.01 M NaOH (the results are not shown here).

370 To estimate maximum amount of HS which can be immobilized onto the solid support with a
371 use of the HS-SQ networks under study, we conducted batch sorption experiments with silica gel
372 (the isotherms are shown in Fig. S1 in the SI). The estimated values of sorption capacity were as
373 high as 200 mg of HS per 1g of silica gel which corresponds to 9% of organic carbon. These
374 estimates are similar to those reported for silanol derivatives in our previous publications.^{7,31} Of
375 even more importance is that they are comparable to those for organic rich geosorbents, such as
376 mollisols, sediments, and others.³² Hence, the developed water-based HS-SQ networks might be
377 also used as soil meliorants for restoring humus content in the degraded soils.

378

379 4. Conclusions

380 The presented results on the synthesis and fractal properties of the water-based HS-SQ networks
381 provide theoretical basis for the targeted design of the HS-SQ soft materials capable of guided self-
382 assembly aimed at in situ immobilization on granular supports, e.g. sand, under conditions of
383 aqueous solution. Detailed studies using in situ SAXS and TEM on aggregation dynamics of these
384 materials during aging allowed us for the first time to define experimental conditions, which enable
385 immobilization of appreciable amounts of humic materials on sand in the form of HS-SQ networks.
386 These conditions converge to a choice of appropriate aging time of the HS-SQ system for achieving
387 a right level of loosely bound cross-linked aggregates, prior it switches to the condensed state of the
388 surface fractals. Strict observation of these conditions is needed to apply the HS-SQ materials as
389 potent remedial agents for installation of injectable humic PRBs. The good prospects are shown for
390 targeted design of the HS-SQ materials with tunable remedial properties aimed at enhancing their
391 performance for the specific applications. For example, for removal of positively charged
392 contaminants (such as cations), the HS-SQ materials with predominant contribution of humic
393 component should be used (e.g., CHP-APTES-50), the sorption of anions is more preferred onto

394 siloxane-rich materials (e.g., CHS-APTES-200), whereas the highest sorption of non-ionogenic
395 hydrophobic compounds is expected onto neutral CHP:APTES networks (e.g., CHP-APTES-100).
396 The immobilized HS-SQ networks can passively intercept and accumulate the pertinent
397 contaminants. Upon exhaustion they can be easily removed by flushing with solution of diluted
398 alkali. Green synthesis, high performance, ease of installation and removal from the solid support
399 are among the most attractive features of these new soft matter agents with promising applications
400 for nature-inspired remedial technologies such as passively PRBs, biomimetic catalysis, and guided
401 self-assembly of polymer-like materials.³³⁻³⁴ They can be also applied for advanced soil restoration
402 and carbon sequestration technologies implying a use of humics-based systems.³⁵

403

404 **Electronic Supplementary Information**

405 The data are provided on impact of different reaction parameters on fractal properties of HS-SQ
406 network over aging in Tables S1 – S4. The sorption protocols and isotherms of the HS-SQ networks
407 immobilization on silica gel are given (Fig. S1).

408

409 **Acknowledgements:** The authors would like to acknowledge Dr. Vladimir V. Volkov (Institute of
410 Crystallography of RAS) for very helpful discussions on the SAXS results. Alexander Volikov
411 would like to express his gratitude to the program of academic exchanges between Lomonosov
412 Moscow State University and the Karlsruhe Institute of Technologies (KIT) for support of his stay at
413 the Institute of Mechanical Processes of KIT (Germany) where he conducted in situ SAXS
414 experiments. The studies on SAXS data interpretation, synthesis and immobilization of humic-
415 siloxane networks were supported by the Russian Science Foundation (grant #16-14-00167).

416

417

418 REFERENCES

- 419 (1) P. MacCarthy. *Soil Sci.*, 2001, **166**, 738-751.
- 420 (2) I.V. Perminova, K. Hatfield and N. Hertkorn. Use of Humic Substances to Remediate
421 Polluted Environments: From Theory to Practice; Springer Verlag, Dordrecht-the Netherlands.
422 2005.
- 423 (3) M. Klučáková. *Environ. Eng. Sci.*, 2014, **31**, 612-620.
- 424 (4) J. Sun and X.A. Zheng, *J. Environ. Monit.*, 2009, **11**, 1801–1809.
- 425 (5) E.H. Owens, G.A. Sergy, C.G. Guenette, R.C. Prince and K. Lee. *Spill Sci. Technol. Bull.*,
426 2003, **8**, 257-272.
- 427 (6) J. Six, E.T. Elliott and K. Paustian. *Soil Biol. Biochem.*, 2000, **32**, 2099-2103.
- 428 (7) A.B. Volikov, V.A. Kholodov, N.A. Kulikova, O.I. Philippova, S.A. Ponomarenko, E.V.
429 Lasareva, A.M. Parfyonova, K. Hatfield and I.V. Perminova. *Catena*. 2016, **137**, 229-236.
- 430 (8) A.B. Volikov, S.A. Ponomarenko, A.I. Konstantinov, K. Hatfield and I.V. Perminova.
431 *Chemosphere*. 2016, **145**, 83-88.
- 432 (9) A.G.S. Prado, B.S. Miranda and G.V.M. Jacintho. *Surf. Sci.*, 2003, **542**, 276-282.
- 433 (10) A.G.S. Prado, B.S. Miranda and J.A. Dias. *Colloids Surf., A*, 2004, **242**, 137-143.
- 434 (11) G. Szabo, S.L. Prosser and R.A. Bulman. *Chemosphere*, 1990, **21**, 729-739.
- 435 (12) L.K. de Oliveira, E.F. Molina, A.L.A. Moura, E.H. de Faria and K.J. Ciuffi. *ACS Appl.*
436 *Mater. Interfaces*, 2016, **8**, 1478–1485.
- 437 (13) R.H. Karol. Chemical Grouting, 2nd ed. Marcel Dekker, New York. 1990.
- 438 (14) M.J. Truex, E.M. Pierce, M.J. Nimmons and S.V. Mattigod. Evaluation of in situ grouting
439 as a potential remediation method for the Hanford central plateau deep vadose zone. Prepared for the
440 U.S. Department of Energy under Contract DE-AC05-76RL01830. PNNL, Richland, Washington,
441 2011.

- 442 (15) R.H. Baney, M. Itoh, A. Sakakibara and T. Suzuki. *Chem. Rev.* 1995; **95**: 1409-1430
- 443 (16) R. Sodkhomkhum and V. Ervithayasuporn. *Polymer* 2016, **86**, 113-119
- 444 (17) V. Goertz, A. Gutsche, N. Dingenouts and H. Nirschl. *J. Phys. Chem. C*, 2012, **116**,
- 445 26938–26946
- 446 (18) K.D. Keefer and D.W. Schaefer. *Phys. Rev. Let.*, 1986, **56**, 2376-2379.
- 447 (19) P.W. Schmidt. *J. Appl. Cryst.*, 1991, **24**, 414-435.
- 448 (20) P.R. Moses, L.M. Wier, J.C. Lennox, H.O. Finklea, J.R. Lenhard and R.W. Murray. *Anal.*
- 449 *Chem.*, 1978, **50**, 576-585.
- 450 (21) H. Ishida, S. Naviroj, S.K. Tripathy, J.J. Fitzgerald and J.L. Koenig. *J. Polym. Sci., Part B:*
- 451 *Polym. Phys.*, 1982, **20**, 701-718.
- 452 (22) R.L. Wershaw, P.J. Burcar, C.L. Sutula and B.J. Wiginton. *Science* 1967, **157**, 1429-1431.
- 453 (23) P.K. Pranzas, R. Willumeit, R. Gehrke, J. Thieme and A. Knöchel. *Anal. Bioanal. Chem.*,
- 454 2003, **376**, 618-625.
- 455 (24) N.Senesi. *Soil Sci.*, 1999, **164**, 841-856.
- 456 (25) J.A. Rice and J.S. Lin. *Environ. Sci. Technol.*, 1993, **27**, 413-414.
- 457 (26) N. Kloster, M. Brigante, G. Zanini, M. Avena. *Colloid. Surf. A*, 2013, **427**, 76–82.
- 458 (27) P. Schmidt. Use of scattering to determine the fractal dimension. *The Fractal Approach to*
- 459 *Heterogeneous Chemistry*. Wiley Interscience, Chichester, UK, 1989.
- 460 (28) F.D. Osterholtz and E.R. Pohl. *J. Adhes. Sci. Technol.*, 1992, **6**, 127-149
- 461 (29) B. Arkles, J.R. Steinmetz, J. Zazyczny and P. Mehta. *J. Adhes. Sci. Technol.*, 1992, **6**, 193-
- 462 206.
- 463 (30) F. Beari, M. Brand, P. Jenkner, R. Lehnert, H.J. Metternich, J. Monkiewicz and H.W.
- 464 Siesler. *J. Organomet. Chem.*, 2001, **625**, 208–216
- 465 (31) I.V. Perminova, L.A. Karpouk, S.A. Ponomarenko, K. Hatfield, A.I. Konstantinov, N.
- 466 Hertkorn and A.M. Muzafarov. *Colloid Surf. A*, 2012, **396**, 224-232

- 467 (32) S. Endo, P. Grathwohl, S.B. Haderlein and T.C. Schmidt. *Environ. Sci. Technol.*, 2009, **43**,
468 393–400
- 469 (33) K. Hagenhoff, J. Dong, B. Chowdhry, L. Torres and S. Leharne. *Physics and Chemistry of*
470 *the Earth, Parts A/B/C*, 2012, **37-39**, 18-25
- 471 (34) F. Sannino, R. Spaccini, D. Savy and A. Piccolo. *J. Hazard. Mat.*, 2013, **261**, 55-62
- 472 (35) A. Piccolo, R. Spaccini, A. Nebbioso and P. Mazzei. *Environ. Sci. Technol.*, 2011, **45**,
473 6697–6702